100 Gb/s Hybrid Multiband (HMB) CAP/QAM signal transmission over a single wavelength

J. L. Wei, *Member, IEEE*, Q. Cheng, D. G. Cunningham, *Member, IEEE*, R. V. Penty, *Senior Member, IEEE*, I. H. White, *Fellow, IEEE*

***Abstract*—Hybrid Multiband (HMB) CAP/QAM transmitter/receiver systems are proposed for the first time. Simulation results are provided to show the feasibility of 100 Gigabit Ethernet links employing a single laser source transmitting HMB CAP-16/QAM-16, CAP-32/QAM-32 and CAP-64/QAM-64 signals. The proposed hybrid scheme has low sensitivity to directly modulated laser nonlinearities. We found that QAM receivers bring about identical jitter tolerance to ideally phase compensated CAP receivers and QAM receivers are more practical since no phase tracking and compensation are required. Compared with the case of using a standard non phase compensated CAP receiver, the use of the modified QAM-16/32/64 receiver significantly lowers system timing jitter sensitivity in the multiband as well as single band case. Results also show that the use of increasing number of bands causes increased system power margin. For practical jitter conditions of ±6ps, three HMB CAP/QAM systems with optimum band counts are identified to be capable of supporting single laser 100 Gb/s transmission over 15 km SMF.**

***Index Terms*—Carrierless amplitude and phase modulation, Quadrature amplitude modulation, Modulation format, Ethernet networks, Equalizer.**

I. Introduction

THERE has been a continuing increase in bandwidth requirements in local area networks from both individual and enterprise users fueled by bandwidth hungry applications such as high definition TV, video-on-demand, social networking and cloud computing. For single mode fiber (SMF) links, IEEE 802.3 has specified a 100 Gb/s solution which uses four wavelength division multiplexed (WDM) channels [1] with each channel operating at 25 Gb/s. This has the benefit of using available mature WDM technology but has increased overall cost and power dissipation as a result of the number of optoelectronic components used. Therefore, various studies have been carried out on techniques using a reduced optoelectronic component count and simpler optical packaging [2,3]. An efficient approach is to adopt advanced modulation schemes featuring high spectral efficiency so as to use a reduced number of optical channels and simultaneously achieve high bit rates by using relatively low speed electronics and optoelectronic components. For example, the IEEE 802.3 Next Generation (NG) 100 Gigabit Ethernet study group recently investigated pulse amplitude modulation (PAM) schemes to support transmission over 500 m to 2 km lengths of SMF [2,3]. Apart from PAM, more advanced modulation formats including optical orthogonal frequency division multiplexing (OFDM) [4-6], carrierless amplitude and phase (CAP) modulation [4,6,7], as well as electrical duobinary modulation [8] have also been proposed.

The major advantages of optical OFDM and CAP modulation include their improved spectral efficiency and system flexibility in comparison with PAM. Optical OFDM fully leverages advanced digital signal processing (DSP) and thus has already been shown to offer great resilience to linear distortion effects such as fiber dispersion. It has also been implemented in various application scenarios [4-6,9-11]. CAP allows a simpler non-DSP implementation by using analogue transversal filters and hence has the potential of both improved cost and energy efficiency while also having excellent performance [4,6,11]. Moreover, multiband CAP systems have also been shown as efficient solutions due to their improved system flexibility and enhanced tolerance to non-flat channel frequency response [7, 12, 13].

Ethernet typically specifies short-haul applications where direct intensity modulation and direction detection (IMDD) are preferred. In this context, directly modulated lasers (DMLs) exhibit strong nonlinearity such as frequency chirp that degrade system performance significantly. However, optical OFDM and CAP have shown excellent resistance to DML nonlinearities, indicating great potential for short distance applications. For example, it has been shown that 100 Gb/s optical OFDM and CAP using a single DML with less than 20 GHz bandwidth can successfully support transmission over 2 km SMF whilst PAM systems cannot [4]. In this respect, experimental demonstrations have shown that multiband CAP systems can support single laser 100 Gb/s transmission over an IMDD optical link with overall bandwidth of only 14 GHz [7, 13]. Moreover, CAP systems implemented without using analog to digital convertors (ADCs) and digital to analog convertors (DACs) exhibit much better power efficiency than optical OFDM [4] and consume less power than the 4 × 25Gb/s

Manuscript received ?, 2014; Revised ? 2014; Accepted ?, 2014.

J. L. Wei is with ADVA Optical Networking SE, Campus Martinsried, Fraunhoferstrasse 9a, 82152 Martinsried/Munich, Germany (JWei@advaoptical.com).

(J. L. Wei,) Q. Cheng, R.V. Penty and I. H. White (was) are with Centre for Photonic Systems, Electrical Engineering Division, Department of Engineering, University of Cambridge, 9 JJ Thomson Avenue, Cambridge CB3 0FA, UK.

D.G. Cunningham is with Avago Technologies, Framlingham Technology Centre, Station Road, Framlingham, Suffolk, IP13 9EZ, UK.

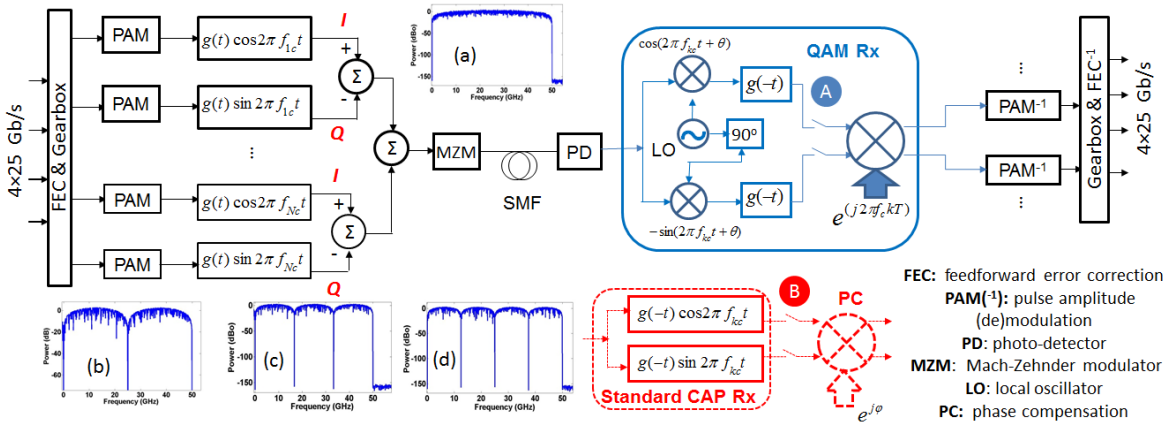

Fig. 1. Diagram of a possible 100G Ethernet PMD enabled by hybrid multiband CAP/QAM transmitters/receivers. For comparison, the standard CAP receivers are also plotted in the red dashed block. As an example, the spectrum of a 100 Gb/s hybrid CAP-16/QAM-16 system is shown in insets with (a) 1 band only, (b) 2 bands, (c) 3 bands and (d) 4 bands. The roll-off coefficient

non-return-to-zero (NRZ) DWDM version of 100G Ethernet [4,6]. These advantages indicate the great potential of multiband CAP systems for high speed optical datacommunications.

The disadvantage of high speed optical CAP data links, however, is their high sensitivity to timing jitter at the receiver as a result of the interference between the two orthogonal channels. As shown later, although a multiband CAP system has larger symbol time period compared to a single band CAP system at the same bit rate, it has even smaller eye width compared with a single band CAP system. As a result, there exists a phase rotation to the recovered constellation diagram when jitter occurs and complex phase tracking and compensation has to be incorporated [7]. However, phase tracking cannot compensate for high frequency jitter that is above the maximum tracking frequency of phase locked loop. Therefore, CAP receivers have relatively low tolerance to high frequency jitter. It is therefore desirable to propose an alternative approach with simple implementations. We have recently shown that single band hybrid CAP/quadrature amplitude modulation (QAM) transmitter/receiver scheme instead of a conventional non phase compensated CAP transceiver [14] can significantly improve not only the system jitter tolerance but also optical link power margin. In this work, for the first time, we propose and theoretically investigate hybrid multiband (HMB) CAP/QAM systems to tackle the practical timing jitter issue that have not received enough attention in previous work [7, 12, 13]. For the first time this paper investigates: the sensitivity of the proposed system to DML nonlinearities, the complexity and efficiency of the multiband CAP system as compared with a QAM or a CAP receiver with or without phase tracking and compensation. It is also found that HMB CAP/QAM systems can further enhance timing jitter tolerance and optical power margin compared with a single band hybrid CAP/QAM.

This paper is organized as follows: Section II presents the principle of proposed 100 Gigabit Ethernet links employing a single laser source and HMB CAP/QAM transmitters/receivers. It also lists the simulation parameters. The use of a phase compensated CAP receiver is also considered via analytical model. The simulated performance of 100 Gb/s hybrid CAP-16/QAM-16, CAP-32/QAM-32, CAP-64/QAM-64 schemes are described and discussed by considering up to four spectral bands in section III. For comparison, the performance of 100 Gb/s multiband CAP transceivers with and without phase tracking and compensation are also investigated in section III. Finally section IV summarizes the work.

II. Principles and System Architectures

A. System Architecture

Fig. 1 shows the block diagram of the 100 Gb/s N-band ($N \geq 1$) hybrid CAP/QAM systems studied here. In the transmitter, the four 25 Gb/s data tributaries are first encoded with FEC and then converted into $2N$ parallel streams. Each tributary stream is mapped into PAM-L (L=4, 6, or 8) symbols and then pulse shaping is performed using a passband square root raised cosine filter [15]. For the k-th (k=1,2,…,N) band, the two shaping filter impulse responses are given by

$$p_{kI}(t) = g(t)\cos(2\pi f_{kc}t) \tag{1}$$

and

$$p_{kQ}(t) = g(t)\sin(2\pi f_{kc}t) \tag{2}$$

where $g(t) = \dfrac{\sin[\pi(1-\alpha)t' + 4\alpha t'\cos[\pi(1+\alpha)t']}{\pi t'[1-(4\alpha t')^2]}$ $\quad t' = t/T$

and $f_{kc} = \dfrac{1}{2T}(1+\alpha)(2k-1)$ is the center frequency of the k-th band, T is the symbol time period and α is the roll-off coefficient. The setting of the center frequency of each band guarantees no spectral overlap between any two adjacent bands. The insets (a)-(d) of Fig. 1 show the spectrum of an example 100 Gb/s CAP-16 signal with 1 to 4 spectral bands. Obviously an N-band CAP system requires $2N$ shaping filters and $2N$ matched filters. The shaped signals of all bands are combined and the resulting signal can be expressed as

$$\begin{aligned} s(t) &= \sum_{k=1}^{N} s_{kI}(t) + s_{kq}(t) \\ &= \sum_{k=1}^{N}\sum_{i=1}[A_{k,i}\,g(t-iT)\cos\omega_{kc}(t-iT) - B_{k,i}\,g(t-iT)\sin\omega_{kc}(t-iT)] \end{aligned} \tag{3}$$

where $\omega_c = 2\pi f_{kc}$ and $A_{k,i}$ ($B_{k,i}$) is the PAM symbol input to the I (Q) channel shaping filter of the *k*-th band at the *i*-th symbol period time. A Mach-Zehnder modulator (MZM) is biased and modulated by the combined multiband CAP signal. The optical signal propagates through a length of SMF and is detected by a square-law photo-detector (PD). The detected electrical signal is then processed in *N* QAM receivers each consisting of two mixers, two baseband matched filters for the in-phase (I) and quadrature (Q) channels, respectively, a local oscillator (LO) and a phase rotator [16]. The LO for the *k*-th band signal has a frequency of f_{kc} . For the electrical back to back case, the *k*-th band recovered I channel signal prior to the phase rotator is given by

$$\begin{aligned} y_{kI}(t) &= [\sum_{j=1}^{N} s_{jI}(t) + s_{jq}(t)]\cos(\omega_{kc}t + \theta) \otimes g(-t) \\ &\cong \sum_i [A_{k,i}\cos(\omega_{kc}iT + \theta) + B_{k,i}\sin(\omega_{kc}iT + \theta)]h(t - iT) \end{aligned} \tag{4}$$

where $h(t) = 0.5[g(t) \otimes g(-t)]$ is a Nyquist pulse. θ is the LO phase used to offset the link delay, which is fixed for a given link. The first term of the right hand side of Eq. (4) contains the transmitted signal from the *k*-th band I channel and the second term contains cross-channel interference (CCI) from the *k*-th band Q channel. Note that the other CCI terms arising from the signals of other bands are filtered out since their frequencies are larger than the bandwidth of the low pass matched filter *g*(-t), and thus not given in Eq. (4). Similarly, the *k*-th band Q channel signal prior to the phase rotator is given by

$$\begin{aligned} y_{kQ}(t) &= [\sum_{j=1}^{N} s_{jI}(t) + s_{jq}(t)] \cdot [-\sin(\omega_{kc}t + \theta)] \otimes g(-t) \\ &\cong \sum_i [B_{k,i}\cos(\omega_{kc}iT + \theta) - A_{k,i}\sin(\omega_{kc}iT + \theta)]h(t - iT) \end{aligned} \tag{5}$$

The phase rotator outputs for the *k*-th band can be expressed by

$$\begin{aligned} A_{k,i}^{'}(t) &= \mathrm{Re}\{[y_{kI}(t) + j \cdot y_{kQ}(t)] \cdot e^{j\omega_{kc}iT}\} \\ &\cong \sum_i A_{k,i}h(t - iT) \end{aligned} \tag{6}$$

and

$$\begin{aligned} B_{k,i}^{'}(t) &= \mathrm{Im}\{[y_{kI}(t) + j \cdot y_{kQ}(t)] \cdot e^{j\omega_{kc}iT}\} \\ &\cong \sum_i B_{k,i}h(t - iT) \end{aligned} \tag{7}$$

After the QAM receiver the PAM signal is decoded, error correction is applied, and the four 25 Gb/s lanes of data are recovered. For comparison, a standard CAP receiver for the *k*-th band is also presented in Fig. 1, which simply consists of two matched filters for the I and Q signal demodulations respectively. The matched filter has a conjugate relationship in the frequency domain compared with its counterpart in the transmitter [15]. The impulse responses of the *k*-th band matched filter pair can be expressed as

$$\tilde{p}_{kI}(t) = g(-t)\cos(2\pi f_{kc}t) \tag{8}$$

and

$$\tilde{p}_{kQ}(t) = g(-t)\sin(2\pi f_{kc}t) \tag{9}$$

The *k*-th band matched filter outputs are given by

$$\begin{aligned} y_{kI}^{'}(t) &= [\sum_{j=1}^{N} s_{jI}(t) + s_{jq}(t)] \otimes [g(-t)\cos\omega_{kc}t] \\ &\cong \sum_i \{A_{k,i}\cos[\omega_{kc}(t - iT)]h(t - iT) \\ &\quad - B_{k,i}\sin[\omega_{kc}(t - iT)]h(t - iT)\} \end{aligned} \tag{10}$$

and

$$\begin{aligned} y_{kQ}^{'}(t) &= [\sum_{j=1}^{N} s_{jI}(t) + s_{jq}(t)] \otimes [g(-t)\sin\omega_{kc}t] \\ &\cong \sum_i B_{k,i}\cos[\omega_{kc}(t - iT)]h(t - iT) \\ &\quad + \sum_i A_{k,i}\sin[\omega_{kc}(t - iT)]h(t - iT) \end{aligned} \tag{11}$$

respectively. The second term of the right hand side of Eq. (10) or (11) represents the CCI, which can only be removed at optimum sampling points (t = i*T*), otherwise the eye exhibits horizontal and vertical closure due to the CCI. However, such CCI does not exist in the modified QAM receiver as indicated in Eq. (6) or (7). It should be noted that other CCI terms from signals of other bands are not listed in Eqs. (10) and (11) since their frequencies are located outside of the passband matched filter spectrum profile.

When a phase estimation is used in a CAP receiver, the CCI term shown in Eqs. (10) and (11) can be removed even if jitter occurs, since the CCI only causes a rotation of constellation diagrams [7]. Suppose the jitter causes a sampling point with offset of τ ($|\tau| < T/2$) relative to the optimum sampling point, namely sampling at t = i($T+\tau$). If a phase correction φ is applied, as shown in Fig. 1, to compensate the constellation rotation, the output samples are given by

$$\begin{aligned} A_{k,i}^{'} &= \mathrm{Re}\{[y_{kI}^{'}(t = \mathrm{i}(\mathrm{T} + \tau)) + j \cdot y_{kI}^{'}(t = \mathrm{i}(\mathrm{T} + \tau))] \cdot e^{j\varphi}\} \\ &= \sum_i \{A_{k,i}\cos[(\omega_{kc}i\tau + \varphi)]h(i\tau) \\ &\quad - B_{k,i}\sin[(\omega_{kc}i\tau + \varphi)]h(i\tau)\} \end{aligned} \tag{12}$$

and

$$\begin{aligned} B_{k,i}^{'} &= \mathrm{Im}\{[y_{kI}^{'}(t = \mathrm{i}(\mathrm{T} + \tau)) + j \cdot y_{kI}^{'}(t = \mathrm{i}(\mathrm{T} + \tau))] \cdot e^{j\varphi}\} \\ &= \sum_i \{B_{k,i}\cos[(\omega_{kc}i\tau + \varphi)]h(i\tau) \\ &\quad + A_{k,i}\sin[(\omega_{kc}i\tau + \varphi)]h(i\tau)\} \end{aligned} \tag{13}$$

respectively. If we set $\varphi = -\omega_{kc}i\tau$, the CCI terms in Eqs. (12) and (13) vanish and Eqs. (12) and (13) come to be identical to Eqs. (6) and (7), respectively if the same jitter is assumed in the QAM receiver. It is clear that the estimated phase rotation is dependent on the timing jitter, it requires phase tracking in practice since jitter is time dependent. On the other hand, there is no phase tracking requirement in a QAM receiver, indicating less complexity for signal recovery. It should be pointed out that in practice, the LO used in a QAM receiver has phase noise which might degrade the system performance to some extent. A jitter cleaner is usually cascaded with a LO so as to eliminate the phase noise effect. Although jitter induced constellation rotation in a CAP receiver can be compensated, there still exists a penalty due to the jittered samples as shown in Eqs. (12) and

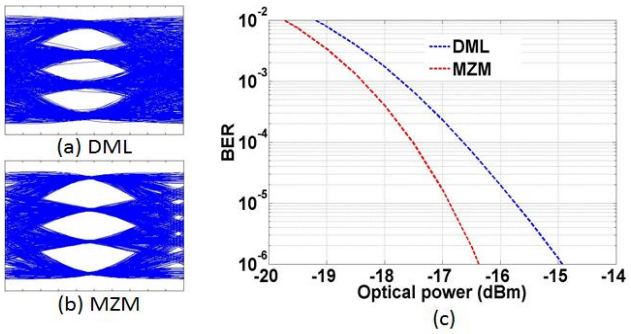

(13). Additionally, high frequency non-data dependent jitter beyond the phase tacking loop bandwidth cannot be tracked or compensated.

As an alternative to the matched filters in the CAP receiver without considering phase compensation, feed forward equalization (FFE) and decision feedback equalization (DFE) may be used to offer channel equalization and demodulation [15]. The remainder of the receiver is identical to that of the conventional CAP receiver after the QAM section.

B. Simulation Parameters

The system transceiver shown in Fig. 1 is modeled assuming an optical transmitter with rise/fall times (20%-80%) of 10 ps, a CW laser operating at 1310 nm with a relative intensity noise (RIN) of -137.3 dB/Hz, a MZM with 3-dB bandwidth (1st order RC response) of 34 GHz, and an optical receiver with a 3-dB bandwidth of 28 GHz. Using this transceiver, a reference 28 Gb/s NRZ signal has a receiver sensitivity of -18 dBm and -14.3 dBm @ BERs of 10^{-3} and 10^{-12}, respectively. The 28 Gb/s reference receiver sensitivity is based on contributions [2,3] to the IEEE NG 100 Gigabit Ethernet Study Group and the IEEE P802.3bm Task Force. However, compared with the current standard, IEEE 802.3ba, the sensitivities are higher by about 3 dBo. Assuming the launch power is set to be 0 dBm, then, by using FEC(10^{-3},10^{-12}) with BER thresholds of 10^{-3}, the total link power budget is $18-5\cdot\log_{10} N$ dB_o for an *N*-band CAP system, assuming that the *N* band signals have approximately equal detected RF powers at the receiver. To achieve this, power loading can be performed in the transmitter to distribute the power between the channels appropriately taking into account the characteristics of the channel frequency loss and the characteristics of the MZM and it electrical drive circuit. The CAP receiver matched filter implementation is determined by the number of CAP bands. For a single (dual) band CAP system, the CAP receiver filter is a 20 (40) tap T/4 (T/8) spaced finite impulse response (FIR) filter and the CAP receiver equalizer consists of a 20 (40) tap T/4 (T/8) FFE and a 3 tap DFE. While for a 3 or 4 band CAP system, the CAP receiver matched filter is an 80 tap T/16 spaced FIR filter and the CAP receiver equalizer consists of an 80 tap T/16 FFE and a 3 tap DFE. Such configuration requires an ADC sampling rate of about 100 GS/s for 100 Gb/s CAP-16 if digital implementation is considered. To perfectly construct the matched filter, oversampling with a factor of 4 was performed. The responsivity for the PD is 0.9A/W and the square root raised cosine shaping filter has a roll-off coefficient of 1.5. The SMF has an attenuation coefficient of 0.5 dB/km. It should be pointed out that most of

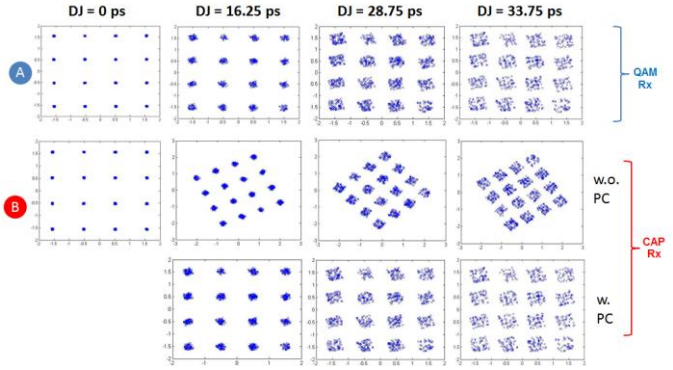

the above listed parameters have been widely used in the published proposals [2, 3].

Unless explicitly stated elsewhere, the above parameters are treated as default values in the paper. In addition, an accurate rate equation based model [4,6] is also used here only for the purpose of examining the impact of DML nonlinearities on the proposed system, as shown in Section III-A.

III. Simulation Results

A. System Resistance to DML nonlinearities

In this section, we examine the sensitivity of the proposed 100 Gb/s HMB CAP/QAM system to DML nonlinearities. In order to identify the impact of DML nonlinearities on the proposed scheme, performance comparisons are made between cases of using DML and using MZM.

Fig. 2 shows the simulated eye diagrams and bit error rate (BER) performance for both cases. The eye diagram of the DML case shows eye closure both horizontally and vertically compared with that of the MZM case. There exists a power penalty of about 0.6 dBo at BER of 10^{-3}, although the power penalty can be very large to achieve a lower BER. The small penalty at the FEC threshold shows that impact of the nonlinearity of the DML on the proposed HMB CAP/QAM system is not significant. This is mainly because each band's CAP signal has a very low symbol rate (6.25 Gbaud for 4-band case without FEC overhead). Simulations also show that when the band count further increases, the proposed scheme has improved resistance to DML nonlinearities simply because of reduced symbol rate for each band.

On the other hand, simulations show that a phase compensated CAP receiver brings about similar sensitivity to the DML nonlinearities compared to the case of using a QAM receiver. However, it is very challenging for a CAP receiver without phase compensation to recover signal properly for both DML and EML cases. The reasons will be presented in detail in the following sections.

B. System Timing Jitter Tolerance with Phase Tracking

As mentioned in Section II, multiband CAP receivers with phase tracking and compensation can mitigate the instrinsic CCI and thus improve timing jitter. This section aims to investigate the ideal performance for CAP receivers using phase compensation and compare it with hybrid multiband CAP/QAM system. Fig. 3 shows the constellation diagrams of a 100 Gb/s 4-band CAP-16 system using QAM-16 receivers and CAP-16 receivers. Although the constellation diagrams are for the 4-th band signals, it is observed in simulations that the performance is similar for the other 3 bands. Fig. 3 shows that

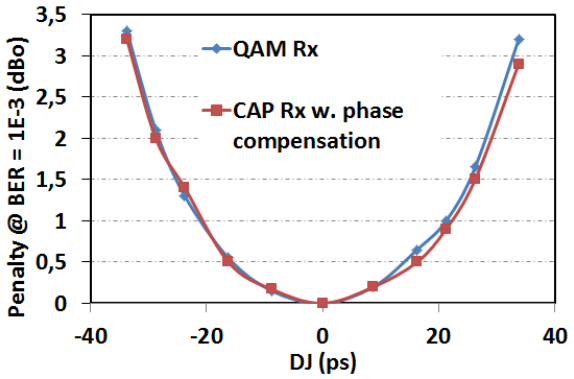

Fig. 4. Penalty versus deterministic jitter for both QAM receiver and CAP receiver cases. For CAP receiver, phase

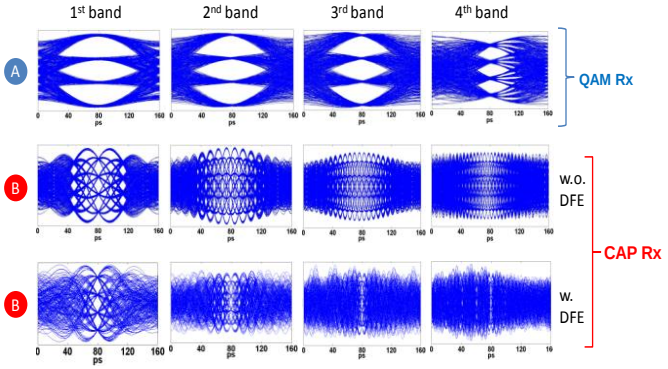

Fig. 5. Noise free eye diagrams of 4-band CAP-16 inphase channels observed at the output of the QAM receivers and the CAP receivers. Both cases of using and not using equalization are considered for CAP receiver. The eye diagrams are

the constellation points split with increasing deterministic jitter (DJ) for both QAM and CAP receivers regardless of phase compensation. In simulations, the sampling points have a time offset corresponding to the DJ relative to the optimum sampling points. For a CAP receiver using no phase compensation, the constellation diagrams also show an increasing phase rotation with growing DJ. This agrees with the theoritical analysis in Section II-A. In contrast, QAM receiver avoids such jitter induced phase rotation. When ideal phase compensation is used in the CAP receiver, the constellation diagrams can be corrected and the corrected diagrams are very similar to those obtained in QAM receivers at the same DJ conditions.

Fig. 4 summarizes the power penalties subject to different DJ conditions for the QAM receiver and the phase compensated CAP receiver. It is not surprising that both receivers show very similar power penalties for a fixed DJ condition. For both cases, the power penalty increases with increasing DJ, which agrees the results shown in Fig. 3. In addition, almost symmetric penalties are observed when the jitter is either positive or negative. This indicates that for DJ within the bandwidth of the pahse tracking loop, phase compensated CAP receivers are equivalent to QAM receivers in terms of deterministic jitter tolerance. However, QAM receivers are more practical since no phase tracking and compensation are required.

C. System Timing Jitter Tolerance without Phase Tracking

In real applications, it might be challenging to implement phase tracking either due to the overhead required or complexity restriction. Thus this section investigates the jitter tolerance for QAM and CAP receiver without using phase compensation.

Fig. 5 shows eye diagrams, constructed from the noise free signal waveforms, of 100 Gb/s 4-band CAP-16 inphase channels observed at the output of both the QAM receivers and the CAP receivers assuming equal received power per channel. The upper row eye diagrams shown in Fig. 5 are for the 1st band to 4th band received inphase signals based on a 4-band hybrid CAP-16/QAM-16 configuration without equalization, while the middle and lower row eye diagrams are their counterparts using CAP receivers. The CAP receiver results are for two cases with the middle row eye diagrams shown in Fig. 5 using matched filters only but with the lower row eye diagrams using FFE and DFE. For all CAP variants, one can see that the QAM receivers bring about much enhanced horizontal eye opening compared with the case using CAP receivers, regardless of whether equalizers are used. This is mainly because, compared with a CAP receiver, the QAM receiver effectively eliminates the inter-channel crosstalk that CAP receivers cannot [14]. This agrees well with the analytical analysis made in Section II. Although the use of FFE and DFE in a CAP receiver improves both the vertical and horizontal eye opening relative to that obtained by a CAP receiver using matched filters only, the improvement is not significant. This is especially the case for CAP schemes with a larger number of amplitude levels where receiver equalizers simply function as matched filters due to their relatively low signal bandwidth.

Fig. 5 also reveals that the eye width (defined as the ratio of time an eye occupies to symbol time period, i.e., unit interval [UI]) of the recovered signal locating at high frequency band is lower than that of the signal of the low frequency band for both QAM and CAP receiver cases. For the QAM receiver case, this trend is due to the limited bandwidth of the overall channel response which causes serious distortion on signals at high frequency band. For the CAP receiver case, this is mainly attributed to the fact that the impulse responses of shaping/matched filters for high frequency band signals have more cycles within one symbol period [12]. In addition, multiband CAP-32 and CAP-64 systems show similar performance to that of CAP-16, although the higher frequency band signal distortion is less significant than that of CAP-16 due to their relatively low signal bandwidth. As a result, the overall system performance of a HMB CAP/QAM system is mainly determined by the signal quality of the highest frequency band channel. In the remainder of this paper, we use the measurement of the highest frequency band channel signal to represent the overall hybrid N-band CAP/QAM system performance.

In order to gain an insight of the relationship between system timing jitter tolerance and band count of multiband CAP systems, Fig. 6 presents the eye diagrams of the recovered inphase signals of a 100 Gb/s CAP-64 system with various band counts. Both QAM receivers and CAP receivers are considered. Note that the eye diagrams are for the highest frequency band only as this represents the worst performance for each case.

In order to gain an insight of the relationship between system

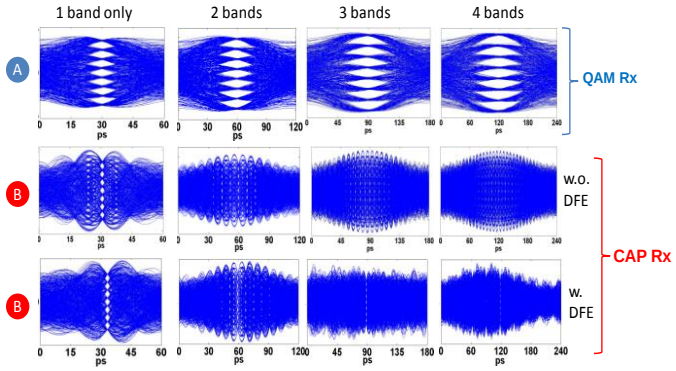

Fig. 6. Noise free eye diagrams of CAP-64 inphase channels with various band counts observed at the output of the QAM receivers and the CAP receivers. Both cases of using and not using DFE equalization are considered for CAP receiver. The eye diagrams are observed at the receiver as marked in Fig.1.

timing jitter tolerance and band count of multiband CAP systems, Fig. 6 presents the eye diagrams of the recovered inphase signals of a 100 Gb/s CAP-64 system with various band counts. Both QAM receivers and CAP receivers are considered. Note that the eye diagrams are for the highest frequency band only as this represents the worst performance for each case. For example, the 3rd (4th) column eye diagrams shown in Fig. 6 are for recovered signals of the 3rd (4th) band signals of a 3(4)-band 100 Gb/s CAP-64 system using either QAM receivers or CAP receivers. It is interesting to note that the eye width from QAM receiver increases with increasing band count, while that from the CAP receiver shows the opposite trend. This is due to the increasing oscillating behaviour of the impulse responses of the CAP receiver matched filters [12], whilst a QAM receiver avoids it by shifting the signal from passband to baseband. Moreover, the symbol period also increases with increasing band count of a CAP system while overall bit rate remains constant. As a result, the HMB CAP/QAM system has great potential in terms of tolerance to jitter. Table I summerizes quantatively the eye widths corresponding to the eye diagrams shown in Fig. 6. It shows clearly that the eye widths of QAM receiver based signals increase almost linearly with band count, while the eye widths of CAP receiver based signals show a slight reduction with increasing band count. One can see that for a practical deterministic jitter (DJ) of >±1 ps required by a typical high speed clock and data recovery (CDR) circuits, conventional CAP receivers are unable to support a single laser 100 Gb/s transmission even if equalization is used. In contrast, HMB

TABLE I
EYE WIDTHS FOR SIGNALS SHOWN IN FIG.6

Band count		1	2	3	4
Symbol period (ps)		60*	120*	180*	240*
QAM Rx	Eye width (UI)	±0.1	±0.12	±0.14	±0.16
	Eye width (ps)	±6	±14.4	±25	±38.4
CAP Rx w/o DFE	Eye width (UI)	±0.016	±0.006	±0.0035	0.0025
	Eye width (ps)	±0.96	±0.72	±0.63	±0.6
CAP Rx w/ DFE	Eye width (UI)	±0.02	±0.006	±0.0036	0.0026
	Eye width (ps)	±1.2	±0.72	±0.65	±0.62

*FEC overhead is not considered.

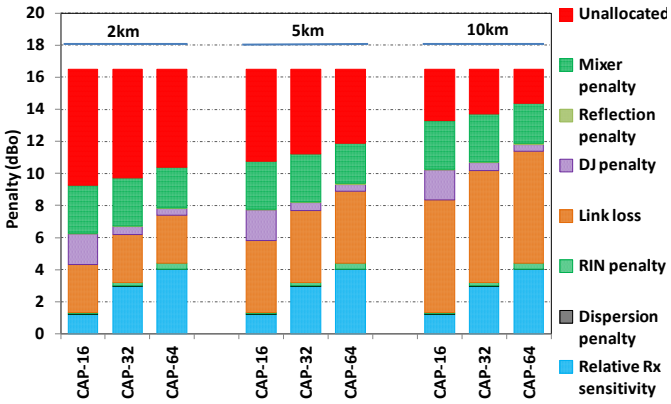

Fig. 7. Link power budget for dual band hybrid CAP-16/QAM-16, CAP-32/QAM-32 and CAP-64/QAM-64

CAP/QAM links offer excellent jitter tolerance under DJ conditions of up to > ±6 ps, which is triple that required by a typical single laser 100 Gigabit Ethernet link that was suggested by the IEEE 802.3 100 Gb/s Optical Ethernet Study Group [2]. It should be noted that the trend shown in Fig. 6 and Table I is also applicable to HMB CAP-16/QAM-16 and CAP-32/QAM-32 systems.

D. Optical Link Power budget

Having shown their strong resilience to timing jitter, this section explores the optical link power budgets for various 100 Gb/s HMB CAP/QAM systems. As an example, Fig. 7 shows the system power budget, assuming equal received modulated power per CAP band, of a 100 Gb/s dual band hybrid CAP-16/QAM-16, CAP-32/QAM-32, and CAP-64/QAM-64 systems. The link power penalty comprises contributions from the relative receiver sensitivity, dispersion penalty, relative intensity noise (RIN) penalty, link loss (fiber attenuation depending on fiber lengths plus 2dB connector loss), DJ penalty, link reflection penalty caused by intermediate connectors [3], mixer penalty, and unallocated penalty if available. The unallocated penalty is a direct indication of the resulting system power margin. If there is a negative unallocated penalty, then the link fails (and no power budget line is shown in the figure). The detailed descriptions of the calculations of each constituent penalty can be found in [4, 6].

It is shown that the three hybrid CAP/QAM systems easily support transmission over 2 km of SMF and that they have enough power margins to achieve transmission over 10 km of SMF. For a fixed fiber length, the achievable power margin is similar for each scheme with CAP-16 exhibiting slightly better margin due to its slightly better receiver sensitivity which is mainly attributed to its having fewer amplitude levels and thus lower multilevel penalty. It should be pointed out that the QAM receivers introduce a mixer penalty of about 3 dBo due to noise amplification from the RF amplifier prior to the mixer. In obtaining Fig. 7, an effective multipath reflection coefficient of -36 dB is assumed for consistency with reference [3] on the basis that there are 10 intermediate connectors in the link. Under this condition, the multipath reflection penalty is negligible for all the schemes. However, it has to be noted that the multipath reflection penalty increases with increasing

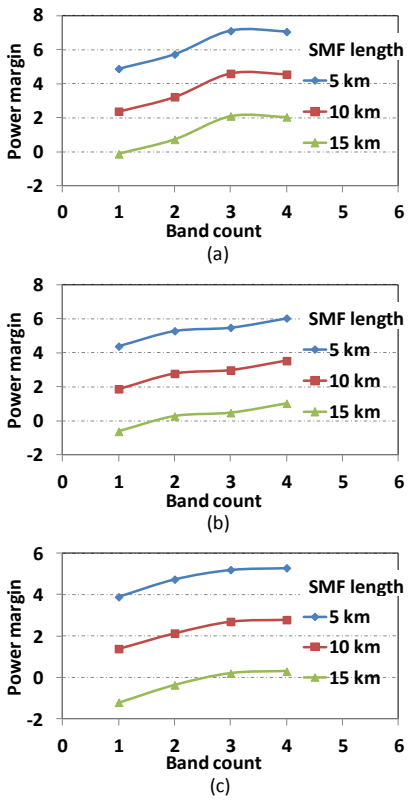

Fig. 8. Achievable system optical power margins for (a) hybrid CAP-16/QAM-16, (b) hybrid CAP-32/QAM-32, and (c) hybrid CAP-64/QAM-64 versus band count under

multipath reflection coefficient [7]. Take the case of hybrid dual band CAP-16/QAM-16 for example, the multipath reflection penalty at a BER of 10^{-3} increases from 0.1 dB to 0.5 dB by increasing the coefficient from -36 dB to -30 dB. In respect of system timing jitter tolerance, a DJ of ±6 ps is considered for all schemes shown in Fig. 7. Under such a condition, Fig. 7 shows the DJ penalty is dependent on the modulation order of a hybrid dual band CAP/QAM link: the higher the modulation order, the less the DJ penalty. This is simply because a higher modulation order brings about larger symbol period time. Fig. 7 also shows that the RIN penalty at 10^{-3} is almost negligible for all schemes with a larger penalty being observed for a scheme with higher modulation order as it has the largest number of amplitude levels. It should be pointed out that RIN penalty is dependent on the timing jitter. As an example, the RIN penalty of the hybrid dual band CAP-64/QAM-64 increases from 0.3 dB to 0.5 dB with increasing DJ from ±6 ps to ±9 ps. This is mainly attributed to the increasing inter symbol interference.

It should be noted that when a CAP receiver is employed with phase tracking and compensation, for jitter that is within the tracking loop bandwidth, the achievable system optical power margin is similar to that of using a QAM receiver as shown in Fig. 7. This is because, first, the DJ tolerance of a phase compensated CAP receiver is similar with a QAM receiver; and second, although there is no mixer penalty for a CAP receiver, it has about 3 dB more noise penalty than QAM receiver case due to that a passband matched filter has a bandwidth two times that of a baseband matched filter.

Fig. 8 shows the achievable system optical power margins for the proposed three hybrid CAP/QAM schemes considering band count up to 4 under different SMF lengths. Once again, equal received modulated power per CAP band is assumed. In obtaining Fig. 8, a DJ of ±3 ps (±6 ps) is considered for the band count of 1 (>1) cases. The other parameters are the same as those of Fig. 7. It can be seen that the system optical power margin increases with increasing band count until it exceeds a threshold value. This is mainly because a high band count brings about significant decrease in DJ penalty as a result of increased eye width and symbol period as shown in Fig. 6. Take hybrid CAP-16/QAM-16 as an example, when the band count increases from 2 to 3 and 4, the DJ penalty decreases from 1.9 dBo to 0.7 dBo and 0.35 dBo. In addition, a high band count also enables a lower relative receiver sensitivity mainly due to the receiver baseband matched filters filtering out more noise. Such relative receiver sensitivity improvement approximately offsets the reduction in per band launch power considering a fixed total optical launch power of 0 dBm, i. e. the SNR per CAP band is independent of band count. However, as the band count exceeds a threshold value, the optical power margin begins to saturate or even drop. This can be explained by two factors: first, the DJ penalty drop is not significant by further increasing band count. Second, a high band count means the channel at the highest frequency band experiences strong distortion as illustrated in Fig. 5 as it falls into the roll-off region of the limited overall channel frequency response. This leads to reduced eye width and increased ISI. Therefore, for practical implementation, it is worth to choose an optimum band count to maximize the system performance.

Fig. 8 also shows that HMB CAP/QAM system enable single laser 100 Gb/s data transmission over 15 km SMF, while hybrid single band CAP/QAM schemes fail. For example, hybrid 3-band CAP-16/QAM-16 (hybrid 4-band CAP-64/QAM-64) supports 15 km SMF transmission with an optical power margin of 2.1 dBo (0.3 dBo). This indicates the great potential of HMB CAP/QAM for high speed datacommunications.

IV. Conclusions

In conclusion, simulations have investigated a single laser 100 Gigabit Ethernet link using HMB CAP-16/QAM-16, CAP-32/QAM-32 and CAP-64/QAM-64 transmitter/receiver. The proposed scheme has low sensitivity to DML nonlinearities. We have shown that QAM receivers are equivalent to phase compensated CAP receivers on aspect of jitter tolerance and QAM receivers are more practical since no phase tracking and compensation are required. Compared with conventional multiband non phase compensated CAP receivers, the use of QAM receivers significantly lowers the system sensitivity to timing jitter. Results show that there exists an optimum band count for each scheme, corresponding to which the system optical margin is maximum. For practical jitter conditions of ±6 ps, these three hybrid scheme with optimum band count are identified to be capable of successfully supporting single laser 100 Gb/s transmission over 15 km of SMF.

It is also worth mentioning that power loading of HMB CAP/QAM systems may be implemented with bit loading as the high frequency band will suffer a severe loss of SNR and bit loading might help make optimum use of the available channel [7]. This will be considered in future experimental work.

ACKNOWLEDGMENT

This work was partly supported by the European Union under a Marie Curie Intra-European Fellowship for Career Development (FP7-PEOPLE-2013-IEF 623515 to J .L. Wei) via the CEEOALAN project and UK Engineering and Physical Sciences Research Council (EPSRC) via the INTERNET project. The authors thank Dr. H. Griesser from ADVA Optical Networking SE for useful discussions. The authors also thank the reviewers for their valuable comments which helped to improve the technical quality of the paper.

REFERENCES

[1] IEEE, IEEE 802.3ba – 40 Gb/s and 100 Gb/s Ethernet, 2010. Standard.
[2] A. Ghiasi, "Investigation of 100 GbE Serial PMDs Based on Advance Modulation," IEEE 802.3 Next Generation 40 Gb/s and 100 Gb/s Optical Ethernet Study Group interim meeting, Jul. 2012.
[3] G. Nicholl, and C. Fludger, "Update on technical feasibility for PAM modulation," IEEE 802.3 Next Generation 40 Gb/s and 100 Gb/s Optical Ethernet Study Group interim meeting, Mar. 2012.
[4] J. L. Wei, J. D. Ingham, R. V. Penty, and I. H. White, "Performance Studies of 100 Gigabit Ethernet Enabled by Advanced Modulation Formats," IEEE 802.3 Next Generation 40 Gb/s and 100 Gb/s Optical Ethernet Study Group interim meeting, May 2012.
[5] W. Yan, T. Tanaka, B. Liu, M. Nishihara, L. Li, , T. Takahara, Z. Tao, J. C. Rasmussen, T.Drenski, "100Gb/s optical IM-DD transmission with 10G-class devices enabled by 65 GSamples/s CMOS DAC Core," Proc. OFC 2013, Paper OM3H.1, (2013).
[6] J. L. Wei, D. G. Cunningham, R. V. Penty, and I. H. White, "Study of 100G Ethernet using carrierless amplitude/phase modulation and optical OFDM," J. Lightwave Technol., 31(9), 1367-1373 (2013).
[7] M. I. Olmedo, T. Zuo, J. B. Jensen, Q. Zhong, X. Xu, S. Popov, and I. T. Monroy, "Multiband Carrierless Amplitude Phase Modulation for High Capacity Optical Data Links," J. Lightw. Technol., vol.32, no. 4, pp. 798-804 (2014) .
[8] J. Lee, N. Kanda, T. Pfau, A. Konczykowska, F. Jorge, J.-Y. Dupuy and Y.-K. Chen, "Serial 103.125 Gb/s transmission over 1 km SSMF for low-cost, short-reach optical interconnects, " OFC 2014, Paper PDP Th5A.5 (2014).
[9] C. Zhang, Q. Zhang, C. Chen, N. Jiang, D. Liu, K. Qiu, S. Liu, B. Wu, "Metro-access integrated network based on optical OFDMA with dynamic sub-carrier allocation and power distribution," Opt. Express, 21(2), 2474-2479 (2013).
[10] E. Giacoumidis, J. L. Wei, X. Q. Jin, and J. M. Tang, "Improved transmission performance of adaptively modulated optical OFDM signals over directly modulated DFB laser-based IMDD links using adaptive cyclic prefix," Opt. Express, Papers 16 (13), 9480-9494 (2008).
[11] J. L. Wei, J. D. Ingham, D. G. Cunningham, R. V. Penty, and I. H. White, "Performance and power dissipation comparisons between 28 Gb/s NRZ, PAM, CAP and optical OFDM systems for datacommunication applications," J. Lightwave Technol., Papers 30(20), 3273-3280 (2012).
[12] J. Zhang, J. Yu, F. Li, N. Chi, Z. Dong, and X. Li, "11 × 5 × 9.3Gb/s WDM-CAP-PON based on optical single-side band multi-level multi-band carrier-less amplitude and phase modulation with direct detection, " Opt. Express, vol. 21, no. 16, pp. 18842-18848 (2013).
[13] T. Zuo, A. Tatarczak, M. I. Olmedo, J. Estaran, J. Bevensee Jensen, Q. Zhong, X. Xu, and I. Tafur, "O-band 400 Gbit/s Client Side Optical Transmission Link," in Optical Fiber Communication Conference, 2014, paper M2E.4.
[14] J. L. Wei, J. D. Ingham, Q. Cheng, D. G. Cunningham, R. V. Penty, and I. H. White, "Experimental Demonstration of Optical Data Links using a Hybrid CAP/QAM Modulation Scheme," Opt. Letters, 39(6), 1402–1405 (2014).
[15] J. J. Werner, *Tutorial on carrierless AM/PM*, ANSI X3T9.5 TP/PMD Working Group, (1992&1993).
[16] W. Y. Chen, G.-H. Im, and J. J. Werner, "Design of digital carrierless AM/PM transceivers," AT&T and Bellcore contribution to ANSI T1E1.4/92-149, (1992).

Jinlong Wei (S'09–M'11) received his PhD degree in Electronic Engineering from Bangor University, Bangor, UK in 2011. He joined the University of Cambridge, Cambridge, UK as a research associate in Aug. 2011 and worked on high-speed energy efficient optical communication systems. He was awarded a Marie Curie grant and joined ADVA Optical Networking SE as a senior engineer in Sept. 2014. He has authored/co-authored over 70 journal and conference publications and held 7 patents.

Qixiang Cheng received the B.Sc. degree in opto-electronics from the Huazhong University of Science and Technology, Wuhan, China in 2010. He is currently a PhD student at the Centre for Photonic Systems, Department of Engineering, University of Cambridge, UK. He has over 20 journal and conference publications and his current research interests include energy efficient Datacommunicaitons and optical switching.

David G. Cunningham is an Avago Technologies R&D Fellow. He received his Ph.D. in Laser Physics from The Queens University, Belfast, Northern Ireland in 1985. He has worked at British Telecommunications Laboratories, Hewlett-Packard Laboratories, Agilent Technologies and Avago Technologies. The IEEE 802.3 and Fibre Channel (INCITS T11) committees have recognized his contributions to their 100 Mb/s to 32 Gb/s standards. David is currently interested in the application of advanced modulation schemes to multimode fiber links.

Richard V. Penty (M'00–SM'10) is currently the Professor of Photonics at the University of Cambridge, UK, where he received his Ph.D. degree in engineering in 1989 and was a Science and Engineering Research Council Information Technology Fellow. He has published over 800 journal/conference papers. His research interests include high-speed optical communications systems, photonic integration and green photonics. He is the Editor-in-Chief of *IET Optoelectronics Journal* and a Fellow of the Royal Academy of Engineering.

Ian H. White (S'82-M'83-SM'00-F'05) is currently Master of Jesus College, Deputy Vice-Chancellor and Head of Photonics Research at the Engineering Department, University of Cambridge. He received the BA and PhD degrees from the University of Cambridge, UK, in 1980 and 1984, respectively. He has published over 900 journal/conference papers and holds 28 patents. He is a Fellow of the Royal Academy of Engineering, the IEE and the IEEE. He is an Editor-in-Chief of *Electronics Letters*.